crystals

MDPI

Article

Structural and Mechanical Properties of Al-SiC-ZrO_2 Nanocomposites Fabricated by Microwave Sintering Technique

Adnan Khan [1,†], Motasem W. Abdelrazeq [1,†], Manohar Reddy Mattli [1], Moinuddin M. Yusuf [1], Abdullah Alashraf [1], Penchal Reddy Matli [2] and R. A. Shakoor [1,*]

1 Center for Advanced Materials (CAM), Qatar University, Doha 2713, Qatar; samikhanmechanical@gmail.com (A.K.); ma1511475@qu.edu.qa (M.W.A.); manoharreddy892@gmail.com (M.R.M.); moinuddin@qu.edu.qa (M.M.Y.); aa.ashraf@qu.edu.qa (A.A.)

2 Department of Mechanical Engineering, National University of Singapore, Singapore 117576, Singapore; drlpenchal@gmail.com

* Correspondence: shakoor@qu.edu.qa

† Authors with equal contribution.

Received: 4 September 2020; Accepted: 4 October 2020; Published: 6 October 2020

Abstract: In the present study, Al-SiC-ZrO_2 nanocomposites were developed and characterized. Towards this direction, the aluminum (Al) matrix was reinforced with nano-sized silicon carbide (SiC) and zirconium dioxide (ZrO_2), and the mixture was blended using ball milling technique. The blended powder was compacted and sintered in a microwave sintering furnace at 550 °C with a heating rate of 10 °C/min and a dwell time of 30 min. The amount of SiC reinforcement was fixed to 5 wt.%, while the concentration of ZrO_2 was varied from 3 to 9 wt.% to elucidate its effect on the microstructural and mechanical properties of the developed nanocomposites. Microstructural analysis revealed the presence and uniform distribution of reinforcements into the Al matrix without any significant agglomeration. The mechanical properties of Al-SiC-ZrO_2 nanocomposites (microhardness and compressive strength) were observed to increase with the increase in the concentration of ZrO_2 nanoparticles into the matrix. Al-SiC-ZrO_2 nanocomposites containing 9 wt.% of ZrO_2 nanoparticles demonstrated superior hardness (67 ± 4 Hv), yield strength (103 ± 5 MPa), and compressive strength (355 ± 5 MPa) when compared to pure Al and other compositions of the synthesized composites. Al-SiC-ZrO_2 nanocomposites exhibited the shear mode of fracture under compression loadings, and the degree of deformation was restricted due to the work hardening effect. The appealing properties of Al-SiC-ZrO_2 nanocomposites make them attractive for industrial applications.

Keywords: microwave sintering; nanocomposite; microstructure; hardness; compressive strength

1. Introduction

In recent years, active research has been in progress to overcome the limitations of monolithic materials and to develop cost-effective smart materials with promising properties to meet modern engineering and industrial requirements [1]. In such applications, aluminum metal matrix composites (AMMCs) are attractive due to their appealing properties such as their low density, high elastic modulus, excellent thermal stability, and wear resistance [2–5]. AMMCs have proven to be one of the most promising structural materials comprising various reinforcements such as silicon carbide (SiC) [6], silicon nitride (Si_3N_4) [7], aluminum oxide (Al_2O_3) [6], yttrium oxide (Y_2O_3) [8–10], boron carbide (B_4C) [11], titanium carbide (TiC) [12], zirconia (ZrO_2) [13], etc.

Recently, Al-based nanocomposites have been considered to be better substitutes for the conventional Al alloys and AMMCs because of their multifunctionality and superior properties [14,15].

Al-based nanocomposites are a new class of composites comprised of a combination of one or more types of nano reinforcements incorporated into the Al matrix, enabling them to make use of the unique properties of individual contributing nano reinforcements [16]. The satisfactory structural performance and promising properties (thermal and mechanical) of Al-based nanocomposites are significantly contributing to a rapid improvement in their popularity and a dramatic widening in their scope of applications [17–20]. As a comparison, Al-based nanocomposites demonstrate superior properties, such as high strength, crack propagation resistance, and more remarkable plasticity at higher loads when compared with conventional composites [21]. Moreover, nanocomposites provide increased design diversity for the selection of materials to satisfy the application requirements [22]. The favorable structural, thermal, mechanical, and multifunctional characteristics of nanocomposites have been well explored in many applications like automobile, aerospace, aeronautical, marine, and other engineering applications [23–28].

In developing Al-based nanocomposites, fabricating techniques play a vital role. It is well documented that fabrication techniques have a significant influence on the strength and structural properties of nanocomposites. Many processes can be used for the synthesis of Al-based nanocomposites, such as powder metallurgy, forging, stir casting, etc. [12,29]. Among these techniques, the powder metallurgy (PM) route tends to be more attractive due to its simplicity, low cost, and the properties it imparts into the developed nanocomposites. Furthermore, in the PM synthesis technique, various sintering techniques are used, including microwave, vacuum, spark plasma, conventional sintering processes, etc. [30–32]. The sintering technique has a significant influence on the microstructural and mechanical properties of the final composites [33]. In comparison with other sintering techniques, the microwave sintering approach is the most effective technique in synthesizing Al-based nanocomposites. In addition to a green source of energy, uniform heating, and improved densification, microwave sintering results in much mor refined grain sizes because of its high heating rate and shorter soaking time, which significantly influences the properties of nanocomposites.

Some nanocomposites have already been developed through different synthesis techniques and reported in the literature. M. Sambathkumar et al. [34] developed Al-SiC-TiC nanocomposites and investigated the influence of reinforcements on their mechanical and anticorrosion properties. Johny James et al. [35] employed the stir casting technique to fabricate Al-based nanocomposites using ZrO_2 and Al_2O_3 as reinforcements and reported improved mechanical properties. Sajjad Arif et al. [36] employed the PM route coupled with a tubular electric furnace in an argon atmosphere for synthesizing Al-SiC-ZrO_2 nanocomposites and concluded that the developed nanocomposites displayed enhanced wear resistance and mechanical properties. K. Sekar et al. [37] utilized stir and squeeze casting techniques to develop Al-SiC-ZrO_2 nanocomposites and conducted a focused study on their welding and mechanical properties. Vinod Kumar et al. [38] studied the effect of ZrO_2 particles on the characteristics of Al-SiC metal matrix composites developed through the stir casting method and reported the impact of the concentration of ZrO_2 particles on the laser machining.

Based on the existing literature, although Al-SiC-ZrO_2 nanocomposites have been previously developed, to the best of our knowledge, the synthesis of Al-SiC-ZrO_2 nanocomposites using the microwave sintering technique has not been reported so far. Since the microwave sintering technique has a significant influence on the structural, thermal, and mechanical properties of Al-based composites, it is thus realistic to explore the development of Al-SiC-ZrO_2 nanocomposites through the microwave sintering technique and to investigate the associated properties. Moreover, to rectify the lack of reports on the effect of the concentration of ZrO_2 on the mechanical behavior of Al-based nanocomposites, a detailed analysis of the impact of the concentration of ZrO_2 on the structural, morphological, and mechanical properties of Al-SiC-ZrO_2 nanocomposites is also reported in the present study. This will be the first report that describes the synthesis and characterization of Al-SiC-ZrO_2 nanocomposites developed through the microwave sintering approach. The desirable properties of Al-SiC-ZrO_2 nanocomposites justify their development and their potential industrial application.

2. Materials and Methods

Pure Al (with 99.5% purity, 10 µm average particle size, Alfa Aesar, Tewksbury, MA, USA) was used as the matrix material. SiC (45–55 nm particle size, purity >99%, Alfa Aesar, Tewksbury, MA, USA) and ZrO_2 (15 nm particle size, 99.7% purity, Alfa Aesar, Tewksbury, MA, USA) particles were used as reinforcing materials. The compositions of pure Al and reinforced materials are shown in Table 1. The samples of nanocomposites materials were fabricated by powder metallurgy method involving ball milling and the microwave sintering process.

Table 1. The composition ratio of the Al-SiC-ZrO_2 nanocomposites.

S. No:	Samples Name	Compositions
1	A1	Pure Al
2	A2	Al-5wt.%SiC
3	A3	Al-5wt.%SiC-3wt.%ZrO_2
4	A4	Al-5wt.%SiC-6wt.%ZrO_2
5	A5	Al-5wt.%SiC-9wt.%ZrO_2

The stoichiometric amounts of the matrix (Al) and reinforcements (SiC, ZrO_2) were weighed carefully using an analytical balance (Sartorius, ENTRIS64-1S, Lower Saxony, Germany). The weighed powders were blended at a speed of 200 rpm for 12 0min using a planetary ball mill PM200 (RETSCH 20.640.0001, Haan, Germany). The blended powder weighing ~1.0 g was compacted into cylindrical pellets at an applied pressure of 50 MPa for 60 sec. Then, the green pellets were sintered using a microwave sintering furnace (VB ceramic furnace, VBCC/MF/1600 °C/14/15, Chennai, India). The furnace has a designed maximum temperature of 1600 °C with high-grade alumina insulation. This type of insulation helps the furnace have a fast rate of heating and serving for severe thermal shock heating cycles. The compacted cylindrical pellets were sintered in a microwave sintering furnace at 550 °C with a heating rate of 10 °C/min and a dwell time of 30 min. Following the pre-determined time in the microwave, the billet was allowed to cool to room temperature without any holding time under ambient atmospheric conditions. The sintering temperature of the billets was determined using a non-contact IR in the microwave sintering furnace. Figure 1 shows the schematic representation of the experimental procedure of the developed nanocomposites.

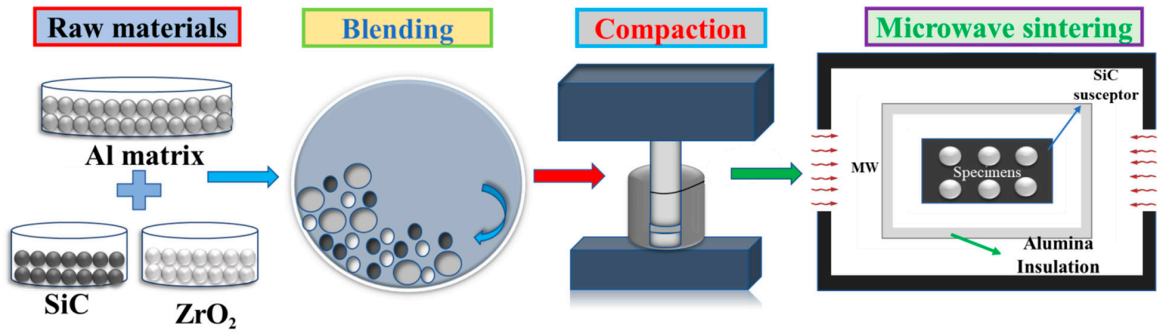

Figure 1. Schematic representation of the development of Al-SiC-ZrO_2 nanocomposites.

The XRD (X-ray diffraction) analysis was performed on the microwave sintered samples (PANalytical X'pert pro, PANalytical B.V., Almelo, The Netherlands), with a scanning rate of 1.5°/min and step size of 0.02° recorded in the 2θ range of 20–80°. The morphological analysis was performed using Field-Emission scanning electron microscope (SEM-FEI Nova NanoSEM 450 FE-SEM, Hillsboro, OR, USA) analysis. The compositional analysis was conducted with energy-dispersive X-ray spectroscopy (Bruker SDD-EDS, Coventry, UK). The surface morphology of the developed Al-SiC-ZrO_2 nanocomposites was studied by using an atomic force microscope (AFM, model MFP-3D, Asylum Research, Abingdon, Oxford, UK).

The relative density of the microwave sintered samples was measured using Archimedes' principle. An analytical balance with density determination equipment (Sartorius YDK03, Lower Saxony, Germany) with an accuracy of ±0.0001 g was used. The microhardness of the Al-SiC-ZrO_2 nanocomposites was determined by using a Vickers microhardness tester (FM-ARS9000, MKV-h21, Tokyo, Japan) with an applied load of 25 gf for 10 sec. The experiment was conducted at room temperature and reported values are an average of five successive indentations for each sample.

The compressive strength of Al-SiC-ZrO_2 nanocomposites analysis was determined at room temperature using a universal testing machine (Lloyd, USA-LR50Kplus, Sussex, UK) applying an engineering strain rate of 10^{-4} s^{-1} under uniaxial compression loadings. The reported values are an average of three successive values of test results. The fractographic analysis was carried out to study the deformation behavior of Al-SiC-ZrO_2 nanocomposites using a field emission scanning electron microscope (SEM-FEI Nova NanoSEM 450 FE-SEM, Hillsboro, OR, USA).

3. Results and Discussion

3.1. XRD Analysis

Figure 2 shows the X-ray diffraction patterns of the microwave sintered pure Al and the developed nanocomposites containing various concentrations of ZrO_2. The results confirm the presence of Al (high-intensity peaks) and reinforcements (SiC and ZrO_2) in the nanocomposites. The intensity of the reinforcement peaks is minimal as compared to the matrix due to their small volume fraction and may be below the detectable limit of the XRD technique [39]. However, with a further increase in the concentration of the reinforcement, an increment in the peak intensities can be noticed, enabling its appearance in the XRD spectra. For more clarity, the enlarged XRD pattern of A5 nanocomposites is also presented in Figure 2b, which confirms the presence of Al, SiC, and ZrO_2 in the matrix, as represented by different symbols [36,40]. These XRD patterns demonstrate that no other phases or impurities are present, which confirms the high purity of the fabricated nanocomposites.

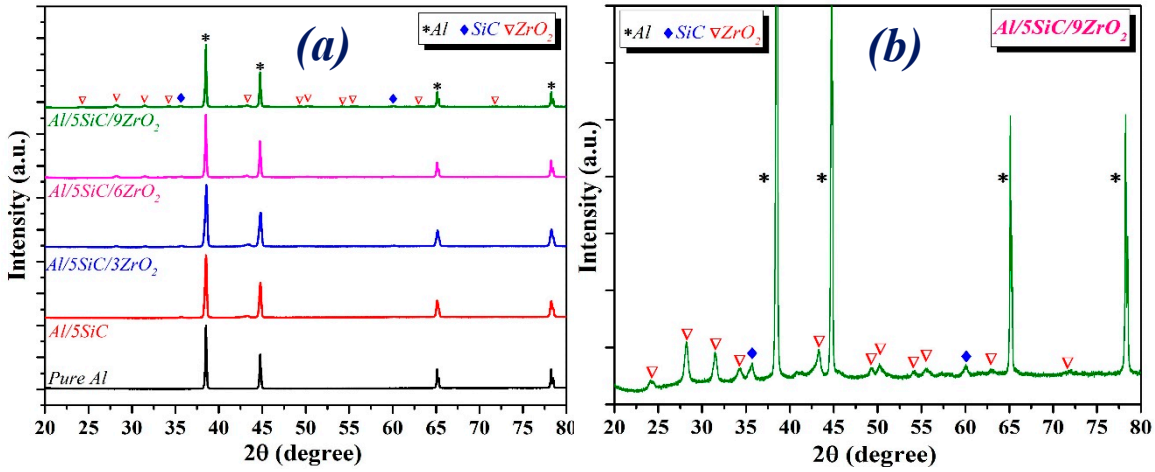

Figure 2. X-ray diffraction patterns (**a**) of developed Al-SiC-ZrO2 nanocomposites and (**b**) an enlarged pattern of Al-5SiC-9ZrO_2 nanocomposites.

3.2. Microstructural Analysis

Figure 3 represents FE-SEM images for microwave sintered nanocomposites with different amounts of reinforcement. It can be observed that the reinforcements (SiC and ZrO_2) are homogeneously distributed in the Al matrix without any significant agglomeration. The homogeneity and the amount of ZrO_2 in the Al matrix have a substantial influence on the microstructure and mechanical properties of the nanocomposites. The presence of ZrO_2 nanoparticles (white color) and SiC (light grey) in the

Al matrix (dark grey) shows the interfacial integrity and confirms the presence of reinforcement. The FE-SEM results are consistent with our XRD results presented in Figure 2.

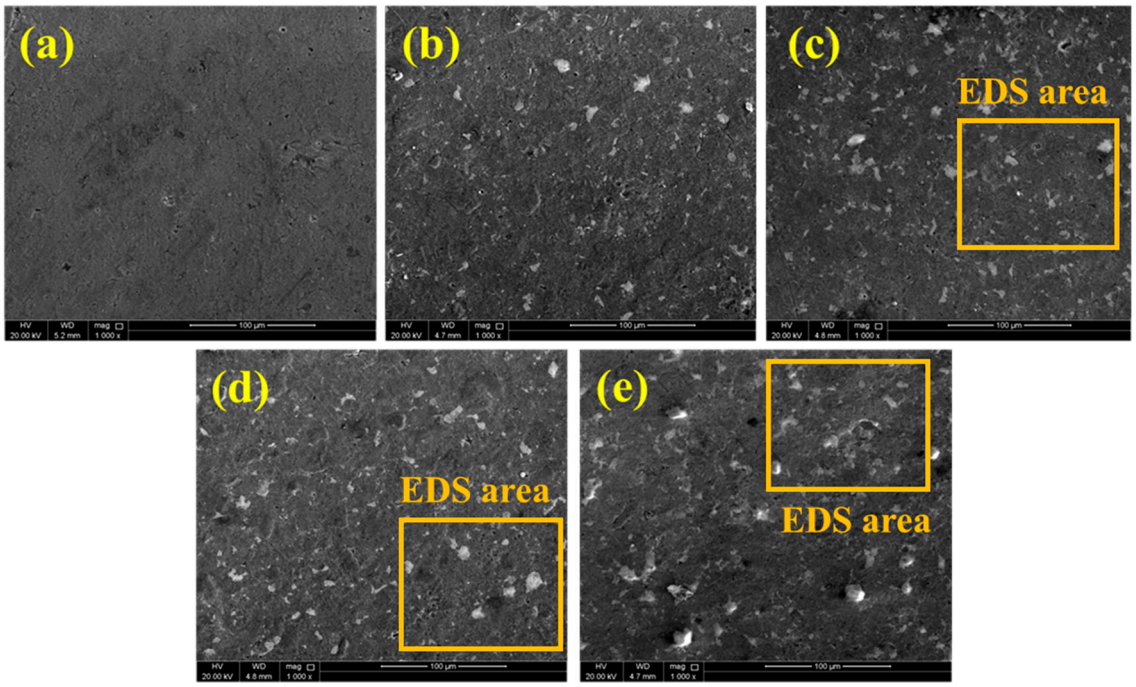

Figure 3. FE-SEM images of (**a**) pure Al, (**b**) Al-5SiC, (**c**) Al-5SiC-3ZrO_2, (**d**) Al-5SiC-6ZrO_2, and (**e**) Al-5SiC-9ZrO_2 nanocomposites with marked areas for energy dispersive X-Ray spectroscopy (EDS).

The energy-dispersive X-ray (EDX) analysis and elemental mapping of the Al-SiC-ZrO_2 nanocomposites (A3, A4, and A5) are presented in Figure 4. The EDX and elemental mapping results confirm the uniform distribution of Si, C, Zr, and O elements in the Al matrix. The EDX spectra in Figure 4 also proves the presence of Al, Si, C, Zr, and O elements in the Al-SiC-ZrO_2 nanocomposites.

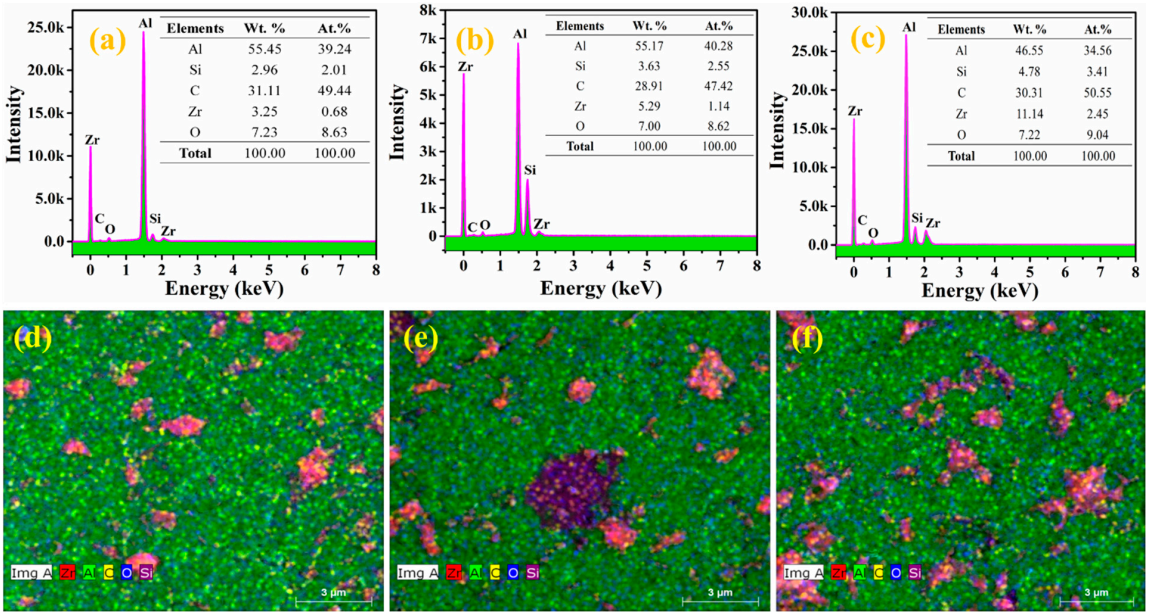

Figure 4. (**a**–**c**) Energy-dispersive X-ray spectroscopy (EDX) spectrum and (**d**–**f**) elemental mapping of Al-5SiC-3ZrO_2, Al-5SiC-6ZrO_2, and Al-5SiC-9ZrO_2 nanocomposites respectively.

3.3. AFM Analysis

Atomic force microscopy (AFM) was utilized to measure the surface properties such as the morphology and surface roughness of the developed nanocomposites. Figure 5 presents the 2D images and X-profile of the developed nanocomposites, as well as the corresponding measured surface roughness. The surface roughness was measured in terms of average roughness (R_a) and root-mean-square (RMS) roughness. The Ra of pure Al is 21.793 nm, however, by adding SiC and ZrO_2 nanoparticles, a gradual increase in the surface roughness was observed in the fabricated nanocomposites, reaching its terminal value at 51.565 nm in A5. The increase in the roughness of Al-SiC-ZrO_2 nanocomposites may be associated with the incorporation of hard ceramic nanoparticles of SiC and ZrO_2, as observed in FE-SEM analysis presented in Figure 3.

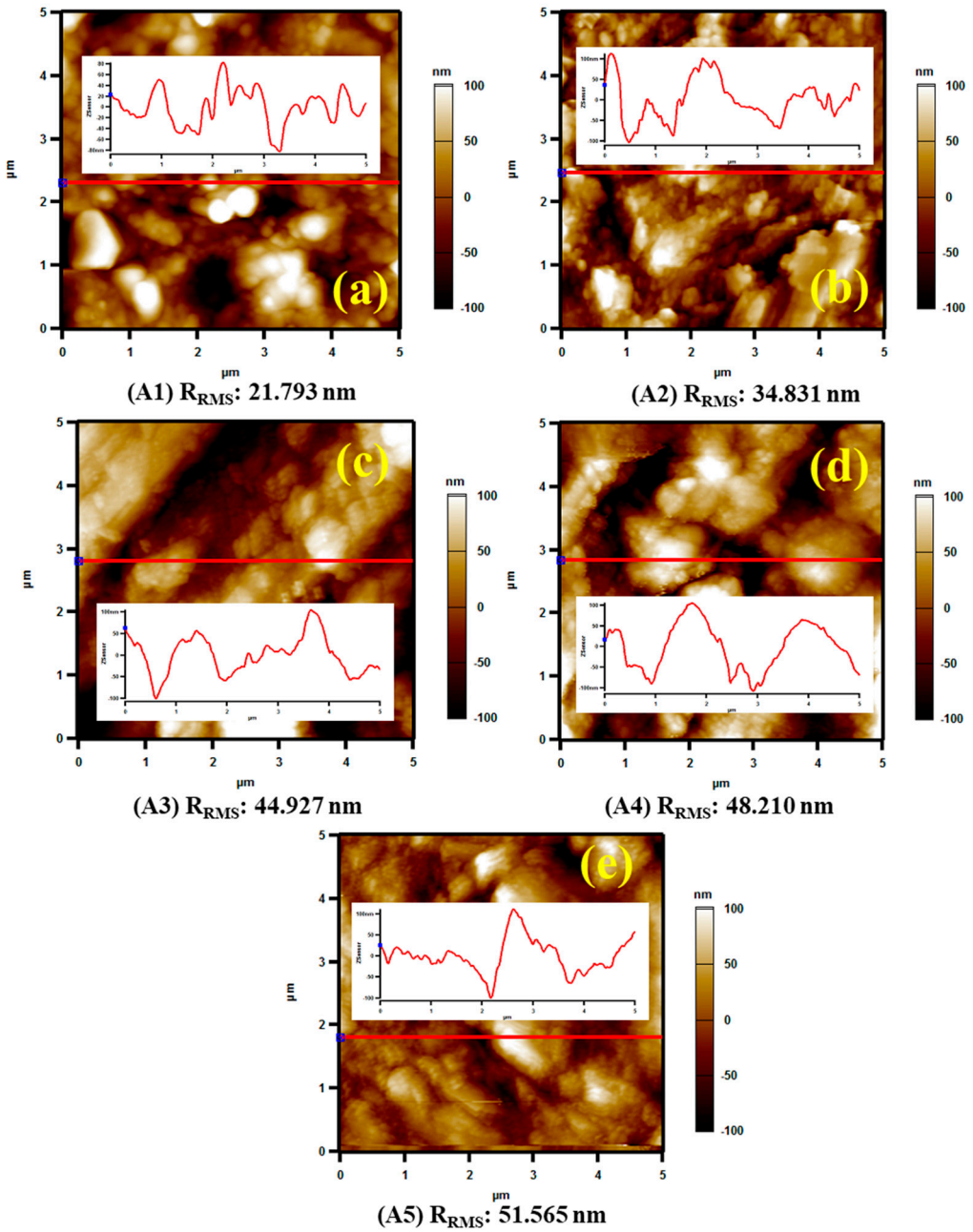

Figure 5. The 2D and X-profile of atomic force microscope (AFM) images of (**a**) pure Al, (**b**) Al-5SiC, (**c**) Al-5SiC-3ZrO_2, (**d**) Al-5SiC-6ZrO_2, and (**e**) Al-5SiC-9ZrO_2 nanocomposites.

3.4. Relative Density and Hardness

Figure 6 shows the relative density and microhardness of the microwave developed Al-SiC-ZrO_2 nanocomposites with different reinforcement contents. It was observed that the relative densities of the nanocomposites increased with an increasing amount of ZrO_2 particles in the matrix. The nanocomposites showed higher relative density than that of their base matrix due to the higher density of the SiC (3.21 g/cm^3) and ZrO_2 (5.68 g/cm^3) as compared to the Al matrix (2.7 g/cm^3). The increasing relative density corresponds to the presence of hard reinforcements, which allows the densification of the reinforcements in the nanocomposites [34]. Figure 6 also shows the variation of the microhardness of the nanocomposites with increases in the ZrO_2 content in the Al matrix, and the corresponding calculated values are tabulated in Table 2. The microhardness results show a decent increase in the microhardness of the developed nanocomposites. The observed microhardness of pure Al is 36 ± 3 HV, which reaches the maximum value of 67± 4 HV for the A5 nanocomposite.

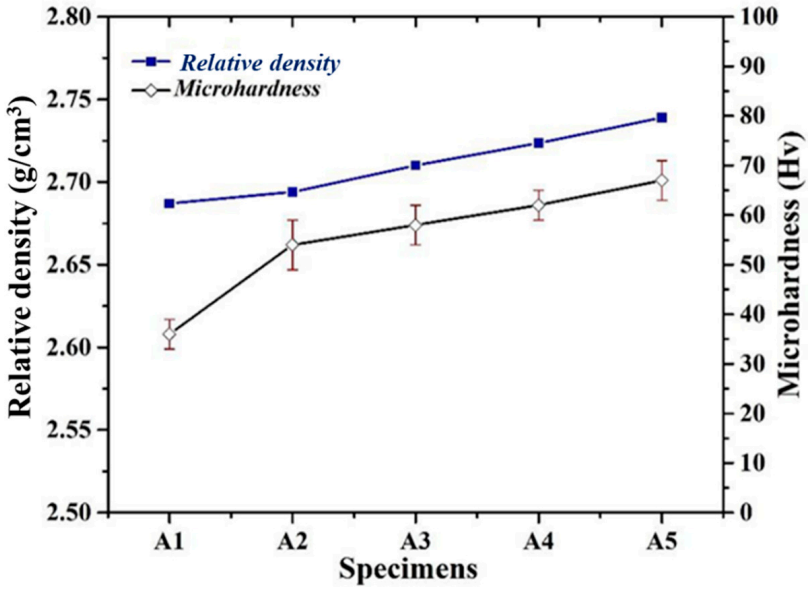

Figure 6. The variation of relative density and hardness of Al-SiC-ZrO_2 nanocomposites with different wt.% of ZrO_2.

This increase in the hardness value of nanocomposites with the increasing amount of ZrO_2 concentration in the Al-matrix can be associated with (i) the presence of hard ceramic particles (SiC and ZrO_2) and their homogenous distribution in Al matrix, (ii) the well-known dispersion hardening effect, (iii) improved densification, which contributes to the increase in hardness, (iv) an improved load-bearing capacity, and (v) strengthening due to the presence of hard particles following the rule of mixture. A similar behavior of the hardness has been reported in previous research [23,41].

3.5. Compressive Analysis

The mechanical properties of the developed nanocomposites were further evaluated by conducting a compressive test at room temperature under uniaxial compressive loading. The engineering stress/strain curves, compressive yield strength (CYS), and ultimate compressive strength (UCS) of pure Al and the developed nanocomposites are presented in Figure 7. Figure 7a indicates the engineering stress/strain curves of the developed nanocomposites. Figure 7b shows the calculated yield strength and compressive strength of the developed nanocomposites from the corresponding engineering stress/strain curves. The calculated mechanical properties of the developed nanocomposites are summarized in Table 2. It can be noticed that the addition of ZrO_2 nanoparticles into the Al matrix leads to increase in the yield strength, and ultimate compression strength of the nanocomposites. As a

comparison, nanocomposites demonstrated improved mechanical properties when compared with Al matrix. Moreover, as shown in Table 2, the A5 sample exhibited the maximum compressive strength of 355 ± 5 MPa with a yield strength of 103 ± 5 MPa at a uniform failure strain of 0.62.

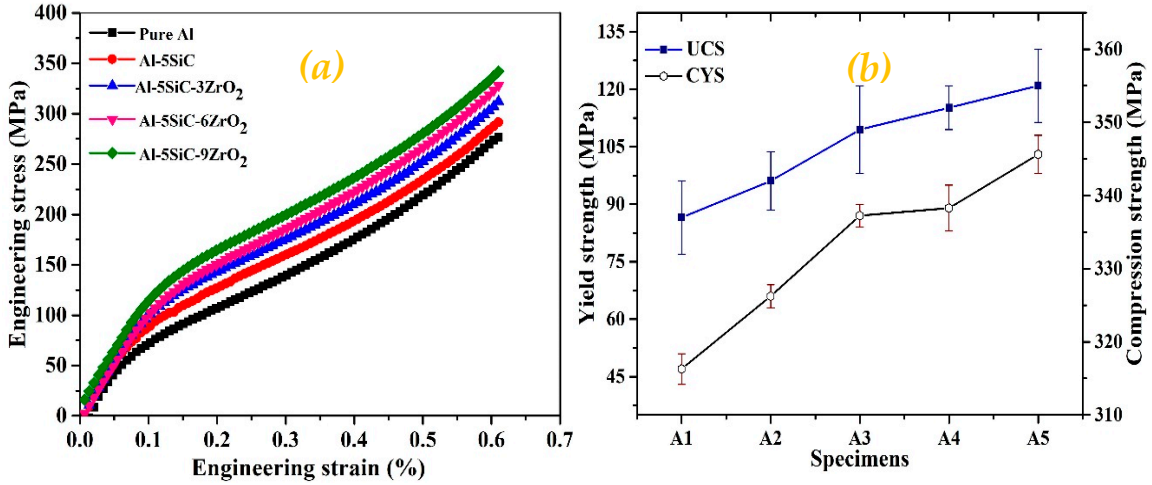

Figure 7. (**a**) Compressive curves, (**b**) compressive yield strength (CYS) and ultimate compressive strength (UCS) of pure Al and the developed Al-SiC-ZrO_2 nanocomposites.

This improvement in the compressive strength of the nanocomposites compared to the Al matrix can be associated with the coupled effect of the presence of hard ceramic nanoparticles, their uniform distribution in the matrix, and the enrichment of the dislocation density due to dispersion hardening effect [11]. There are many reported strengthening mechanisms/theories to explicate the strengthening mechanism in metal matrix composites. In the present study, the strengthening of the fabricated nanocomposites can be explained by considering the most active strengthening mechanism called the dispersion hardening mechanism. Dispersion hardening is also known as Orowan strengthening, which is caused by the hard second phase dispersed in the matrix material. The strengthening effect in the composite materials can be estimated as given by the Orowan–Ashby equation [1,7], which indicates that the smaller particle size of the reinforcement and its large volume fraction will improve the strength of the composite material when keeping all other variables as constant, as is observed in our nanocomposites. A similar observation has been reported in much earlier reports [6].

$$\sigma_{Orowan} = \frac{1}{\lambda}(0.13Gb)\ \ln\left(\frac{r}{b}\right) \quad (1)$$

where λ is interparticle spacing, G is the shear modulus of Al, b is the Burgers vector of Al, and r is the particle radius of the nanoparticle. The interparticle spacing is given by the following equation [42]:

$$\lambda = \frac{4(1-f)r}{3f} \quad (2)$$

where f is the volume fraction of the reinforcement particles.

Table 2. Hardness and compressive properties of Al/SiC/ZrO_2 nanocomposites and their comparison with other nanocomposites.

Composition	Microhardness	Compressive Properties			References
	(Hv)	CYS (MPa)	UCS (MPa)	Failure Strain (%)	
Pure Al	36 ± 3	47 ± 4	337 ± 5	<60	Present work
Al-5SiC	54 ± 5	66 ± 3	342 ± 4	<60	
Al-5SiC-3ZrO_2	58 ± 4	87 ± 3	349 ± 6	<60	
Al-5SiC-6ZrO_2	62 ± 3	98 ± 6	352 ± 3	<60	
Al-5SiC- 9ZrO_2	67 ± 4	103 ± 5	355 ± 5	<60	
Al-1.5Fe_2O_3-2Al_2O_3	47.2	-	152	0.64	[43]
Al-2.5Fe_2O_3-2Al_2O_3	42.9	-	125	0.53	
Al-5RHA-5FA	58.66	-	213	-	[44]
Al-6RHA-4FA	63.0.	-	216	-	
Al-2.5TiO_2-2.5CuO	73	278	250	-	[45]
Al-4Ni-8SiC	48.12	-	-	-	[46]
Al6063-6SiC-2Gr	65.3	-	176	-	[47]
Al6061-7Al_2O_3-20SiC	-	-	300	-	[48]

3.6. Fractography

Figure 8 illustrates the fractographic images of pure Al and Al-SiC-ZrO_2 nanocomposites under compressive loading. The shear mode structure can be observed in both the pure Al and nanocomposites. It can be observed that the occurrence of shear mode fractures in the Al matrix was less compared to its reinforced nanocomposites [49]. Furthermore, due to the work hardening behavior, the degree of compressive deformation that occurred in the pure Al and the nanocomposites is different. The plastic deformation is restricted because of the presence of secondary phases of the reinforcement in the nanocomposites [50].

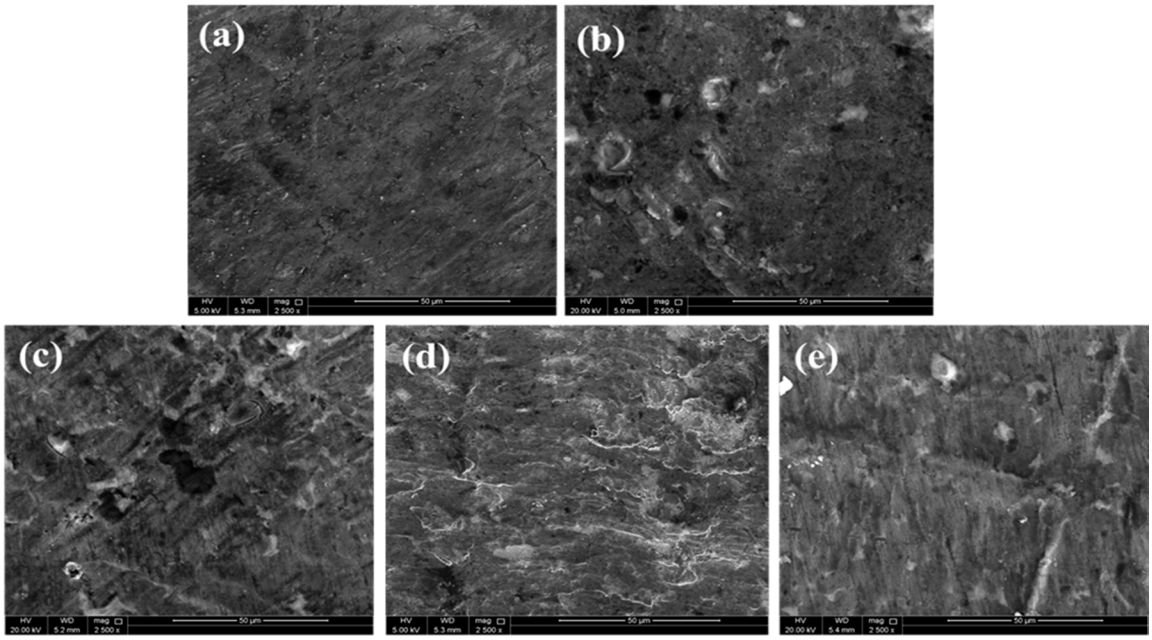

Figure 8. Compression fracture surfaces of (**a**) pure Al, (**b**) Al-5SiC, (**c**) Al-5SiC-3ZrO_2, (**d**) Al-5SiC-6ZrO_2, and (**e**) Al-5SiC-9ZrO_2 nanocomposites.

4. Conclusions

In this study, Al-SiC-ZrO_2 nanocomposites containing a fixed amount of SiC (5 wt.%) and varying concentrations of ZrO_2 (3, 6, and 9 wt.%) were fabricated successfully by powder metallurgy route using the microwave sintering technique. A comparison of mechanical properties indicated that the fabricated nanocomposites demonstrated superior properties when compared to monolithic aluminum (Al). The mechanical properties of the nanocomposites (hardness, yield strength, and compressive strength) increased with an increasing amount of ZrO_2. Al-5SiC-9ZrO_2 showed 119%, and 56% increases in yield strength compared to pure Al and Al-5SiC nanocomposites, respectively. This improvement in mechanical behavior can be attributed to the uniform of hard ceramic nanoparticles (SiC and ZrO_2) and their presence, which activates the dispersion hardening phenomenon.

Author Contributions: A.K. wrote the main part of the manuscript and developed the planning of the experiment. M.W.A. and M.R.M. carried out the preparation of different composite materials and tested physical properties. M.M.Y. and A.A. performed characterization of the microstructure and mechanical studies of the samples. P.R.M. and R.A.S. supervised the materials preparation process and modified the manuscript draft. All authors have read and agreed to the published version of the manuscript.

Funding: This research received no external funding.

Acknowledgments: The authors greatly acknowledge the technical support of the Center for Advanced Materials (CAM), Qatar University, 2713, Doha, Qatar. The FE-SEM and EDX analyses were accomplished at the Central Laboratory Unit (CLU), Qatar University, Doha, Qatar.

Conflicts of Interest: The authors declare no conflict of interest.

References

1. Dieter, G. Mechanical Metallurgy. McGRAW-HILL BOOK COMPANY, US. 1961, pp. 370–371. Available online: http://stu.westga.edu/~{}bthibau1/MEDT%207477-Cooper/Calibre%20Library/Dieter_%20George%20Ellwood/Mechanical%20metallurgy%20(13)/Mechanical%20metallurgy%20-%20Dieter_%20George%20Ellwood.pdf (accessed on 6 October 2020).
2. Song, W.; Veca, L.M.; Anderson, A.; Cao, M.; Cao, L.; Sun, Y. Light-weight nanocomposite materials with enhanced thermal transport properties. *Nanotechnol. Rev.* **2012**, *1*, 363–376. [CrossRef]
3. Khan, A.; Matli, P.R.; Nawaz, M.; Mattli, M.R. Microstructure and Mechanical Behavior of Hot Extruded Aluminum/Tin-Bismuth Composites Produced by Powder Metallurgy. *Appl. Sci.* **2020**, *10*, 2812. [CrossRef]
4. Reddy, M.; Khan, A.; Reddy, P.; Yusuf, M.; Ashraf, A.A.; Shakoor, R.A.; Gupta, M. Effect of Inconel625 particles on the microstructural, mechanical, and thermal properties of Al-Inconel625 composites. *Mater. Today Commun.* **2020**, *25*, 101564.
5. Alem, S.A.A.; Latifi, R.; Angizi, S.; Hassanaghaei, F.; Aghaahmadi, M.; Ghasali, E.; Rajabi, M. Microwave sintering of ceramic reinforced metal matrix composites and their properties: A review. *Mater. Manuf. Process.* **2020**, *35*, 303–327. [CrossRef]
6. Ibrahim, M.A. Mechanical Properties of Aluminium Matrix Composite Including SiC/Al_2O_3 by Powder Metallurgy-A Review. *GSJ J. Public* **2019**, *7*, 23–37.
7. Mattli, M.; Matli, P.; Shakoor, A.; Amer Mohamed, A. Structural and Mechanical Properties of Amorphous Si3N4 Nanoparticles Reinforced Al Matrix Composites Prepared by Microwave Sintering. *Ceramics* **2019**, *2*, 126–134. [CrossRef]
8. Bouaeshi, W.B.; Li, D.Y. Effects of Y_2O_3 addition on microstructure, mechanical properties, electrochemical behavior, and resistance to corrosive wear of aluminum. *Tribol. Int.* **2007**, *40*, 188–199. [CrossRef]
9. Zhao, N.Q.; Jiang, B.; Du, X.W.; Li, J.J.; Shi, C.S.; Zhao, W.X. Effect of Y_2O_3 on the mechanical properties of open cell aluminum foams. *Mater. Lett.* **2006**, *60*, 1665–1668. [CrossRef]
10. Mattli, M.R.; Shakoor, A.; Matli, P.R.; Mohamed, A.M.A. Microstructure and compressive behavior of Al–Y2O3 nanocomposites prepared by microwave-assisted mechanical alloying. *Metals (Basel)* **2019**, *9*, 414. [CrossRef]
11. Ubaid, F.; Matli, P.R.; Shakoor, R.A.; Parande, G.; Manakari, V.; Amer Mohamed, A.M.; Gupta, M. Using B4C nanoparticles to enhance thermal and mechanical response of aluminum. *Materials (Basel)* **2017**, *10*, 621. [CrossRef]

12. Ghasali, E.; Fazili, A.; Alizadeh, M.; Shirvanimoghaddam, K.; Ebadzadeh, T. Evaluation of microstructure and mechanical properties of Al-TiC metal matrix composite prepared by conventional, microwave and spark plasma sintering methods. *Materials (Basel)* **2017**, *10*, 1255. [CrossRef] [PubMed]
13. Patoliya, D.M.; Sharma, S. Preparation and Characterization of Zirconium Dioxide Reinforced Aluminium Metal Matrix Composites. *Eng. Technol.* **2015**, *4*, 3315–3321.
14. Ravichandran, M.; Naveen Sait, A.; Anandakrishnan, V. Al–TiO2–Gr powder metallurgy hybrid composites with cold upset forging. *Rare Met.* **2014**, *33*, 686–696. [CrossRef]
15. Elango, G.; Raghunath, B.K. Tribological behavior of hybrid (LM25Al + SiC+ TiO_2) metal matrix composites. *Procedia Eng.* **2013**, *64*, 671–680. [CrossRef]
16. El Mahallawi, I.; Shash, Y.; Rashad, R.M.; Abdelaziz, M.H.; Mayer, J.; Schwedt, A. Hardness and Wear Behaviour of Semi-Solid Cast A390 Alloy Reinforced with Al_2O_3 and TiO_2 Nanoparticles. *Arab. J. Sci. Eng.* **2014**, *39*, 5171–5184. [CrossRef]
17. Mohapatra, S.; Mishra, D.K.; Mishra, G.; Roy, G.S.; Behera, D.; Mantry, S.; Singh, S.K. A study on sintered TiO2 and TiO2/SiC composites synthesized through chemical reaction based solution method. *J. Compos. Mater.* **2013**, *47*, 3081–3089. [CrossRef]
18. Muley, A.V.; Aravindan, S.; Singh, I.P. Nano and hybrid aluminum based metal matrix composites: An overview. *Manuf. Rev.* **2015**, *2*, 15. [CrossRef]
19. Mahna, S.; Singh, H.; Tomar, S.; Bhagat, D.; Patnaik, A.; Ranjan, S. Dynamic mechanical behavior of nano-ZnO reinforced dental composite. *Nanotechnol. Rev.* **2019**, *8*, 90–99. [CrossRef]
20. Karwowska, E. Antibacterial potential of nanocomposite-based materials—A short review. *Nanotechnol. Rev.* **2017**, *6*, 243–254. [CrossRef]
21. Bodunrin, M.O.; Alaneme, K.K.; Chown, L.H. Aluminium matrix hybrid composites: A review of reinforcement philosophies; Mechanical, corrosion and tribological characteristics. *J. Mater. Res. Technol.* **2015**, *4*, 434–445. [CrossRef]
22. Mohapatra, S. Processing, Microstructure and Properties of Hybrid Metallic and Ceramic Reinforced Aluminium Composites, National Institute Of Technology, Rourkela. 2013. Available online: http://ethesis.nitrkl.ac.in/5362/1/211MM1363.pdf (accessed on 6 October 2020).
23. Madhukar, P.; Selvaraj, N.; Rao, C.S.P. Manufacturing of aluminium nano hybrid composites: A state of review. *IOP Conf. Ser. Mater. Sci. Eng.* **2016**, *149*. [CrossRef]
24. Iacob, G.; Ghica, V.G.; Buzatu, M.; Buzatu, T.; Petrescu, M.I. Studies on wear rate and micro-hardness of the Al/Al2O3/Gr hybrid composites produced via powder metallurgy. *Compos. Part B Eng.* **2015**, *69*, 603–611. [CrossRef]
25. Alizadeh, A.; Abdollahi, A.; Biukani, H. Creep behavior and wear resistance of Al 5083 based hybrid composites reinforced with carbon nanotubes (CNTs) and boron carbide (B4C). *J. Alloys Compd.* **2015**, *650*, 783–793. [CrossRef]
26. Ghasali, E.; Pakseresht, A.H.; Alizadeh, M.; Shirvanimoghaddam, K.; Ebadzadeh, T. Vanadium carbide reinforced aluminum matrix composite prepared by conventional, microwave and spark plasma sintering. *J. Alloys Compd.* **2016**, *688*, 527–533. [CrossRef]
27. Ahlatci, H.; Koçer, T.; Candan, E.; Çimenoğlu, H. Wear behaviour of Al/(Al2O3p+SiCp) hybrid composites. *Tribol. Int.* **2006**, *39*, 213–220. [CrossRef]
28. Zhang, X.N.; Geng, L.; Wang, G.S. Fabrication of Al-based hybrid composites reinforced with SiC whiskers and SiC nanoparticles by squeeze casting. *J. Mater. Process. Technol.* **2006**, *176*, 146–151. [CrossRef]
29. Arif, S.; Alam, M.T.; Ansari, A.H.; Siddiqui, M.A.; Mohsin, M. Investigation of Mechanical and Morphology of Al-SiC composites processed by PM Route. *IOP Conf. Ser. Mater. Sci. Eng.* **2017**, *225*. [CrossRef]
30. Liu, G.; Wang, Q.; Liu, T.; Ye, B.; Jiang, H.; Ding, W. Effect of T6 heat treatment on microstructure and mechanical property of 6101/A356 bimetal fabricated by squeeze casting. *Mater. Sci. Eng. A* **2017**, *696*, 208–215. [CrossRef]
31. Kannan, C.; Ramanujam, R. Comparative study on the mechanical and microstructural characterisation of AA 7075 nano and hybrid nanocomposites produced by stir and squeeze casting. *J. Adv. Res.* **2017**, *8*, 309–319. [CrossRef]
32. Materials, H.; Ghasali, E.; Baghchesaraee, K.; Orooji, Y. International Journal of Refractory Metals Study of the potential effect of spark plasma sintering on the preparation of complex FGM / laminated WC-based cermet. *Int. J. Refract. Metals Hard Mater.* **2020**, *92*, 105328.

33. Ghasali, E.; Orooji, Y.; Niknam, H. Heliyon Investigation on in-situ formed Al 3 V-Al-VC nano composite through conventional, microwave and spark plasma sintering. *Heliyon* **2019**, *5*, e01754. [CrossRef] [PubMed]
34. Sambathkumar, M.A.; Navaneethakrishnan, P.; Ponappa, K.S.K.S. Mechanical and Corrosion Behavior of Al7075 (Hybrid) Metal Matrix Composites by Two Step Stir Casting Process. *Lat. Am. J. Solids Struct.* **2016**, *7075*, 243–255.
35. James, S.J.; Ganesan, M.; Santhamoorthy, P.; Kuppan, P. Development of hybrid aluminium metal matrix composite and study of property. *Mater. Today Proc.* **2018**, *5*, 13048–13054. [CrossRef]
36. Arif, S.; Alam, M.T.; Ansari, A.H.; Siddiqui, M.A.; Mohsin, M. Study of mechanical and tribological behaviour of Al/SiC/ZrO 2 hybrid composites fabricated through powder metallurgy technique. *Mater. Res. Express* **2017**, *4*. [CrossRef]
37. Sekar, K.; Jayachandra, G.; Aravindan, S. Mechanical and Welding Properties of A6082-SiC-ZrO2 Hybrid Composite Fabricated by Stir and Squeeze Casting. *Mater. Today Proc.* **2018**, *5*, 20268–20277. [CrossRef]
38. Kumar, V.; Sharma, V. Effects of SiC, Al_2O_3, and ZrO_2 particles on the LBMed characteristics of Al/SiC, Al/Al2O3, and Al/ZrO2 MMCs prepared by stir casting process. *Part. Sci. Technol.* **2018**, *37*, 770–780. [CrossRef]
39. Lahiri, D.; Singh, V.; Li, L.H.; Xing, T.; Seal, S.; Chen, Y.; Agarwal, A. Insight into reactions and interface between boron nitride nanotube and aluminum. *J. Mater. Res.* **2012**, *27*, 2760–2770. [CrossRef]
40. MA, B.; YU, J. Phase composition of SiC-ZrO2 composite materials synthesized from zircon doped with La2O3. *J. Rare Earths* **2009**, *27*, 806–810. [CrossRef]
41. Singh, J.; Chauhan, A. ARTICLE IN PRESS Characterization of hybrid aluminum matrix composites for advanced applications—A review ARTICLE IN PRESS. *Integr. Med. Res.* **2015**, *5*, 159–169.
42. Ramezanalizadeh, H.; Emamy, M.; Shokouhimehr, M. A novel aluminum based nanocomposite with high strength and good ductility. *J. Alloys Compd.* **2015**, *649*, 461–473. [CrossRef]
43. Alalkawi, H.J.M.; Aziz, G.A.; Aljawad, H.A. Preparation of new aluminum matrix composite reinforced with hybrid nano reinforcements Fe2O3 and Al2O3 via (P/M) route. *Int. J. Mech. Eng. Technol.* **2019**, *10*, 2046–2058.
44. Subrahmanyam, A.P.S.V.R.; Madhukiran, J.; Naresh, G.; Madhusudhan, S. Fabrication and Characterization of Al356.2, Rice Husk Ash and Fly Ash Reinforced Hybrid Metal Matrix Composite. *Int. J. Adv. Sci. Technol.* **2016**, *94*, 49–56. [CrossRef]
45. Ahmadi, M.; Siadati, M.H. Synthesis, mechanical properties and wear behavior of hybrid Al/(TiO_2 + CuO) nanocomposites. *J. Alloys Compd.* **2018**, *769*, 713–724. [CrossRef]
46. Dileep, B.P.; Ravikumar, V.; Vital, H.R. Mechanical and Corrosion Behavior of Al-Ni-Sic Metal Matrix Composites by Powder Metallurgy. *Mater. Today Proc.* **2018**, *5*, 12257–12264. [CrossRef]
47. Bhoria, V.; Suri, N.M. Effect on Mechanical Properties of Aluminium 6063 Reinforced with Silicon Carbide—Graphite Hybrid Composites. *Procedia Eng.* **2016**, *4*, 821–823.
48. Senthil Murugan, S.; Jegan, V.; Velmurugan, M. Mechanical properties of SiC, Al2O3 reinforced aluminium 6061-T6 hybrid matrix composite. *J. Inst. Eng. Ser. D* **2017**, *99*, 71–77. [CrossRef]
49. Matli, P.R.; Ubaid, F.; Shakoor, R.A.; Parande, G.; Manakari, V.; Yusuf, M.; Amer Mohamed, A.M.; Gupta, M. Improved properties of Al-Si3N4 nanocomposites fabricated through a microwave sintering and hot extrusion process. *RSC Adv.* **2017**, *7*, 34401–34410. [CrossRef]
50. Penchal Reddy, M.; Manakari, V.; Parande, G.; Ubaid, F.; Shakoor, R.A.; Mohamed, A.M.A.; Gupta, M. Enhancing compressive, tensile, thermal and damping response of pure Al using BN nanoparticles. *J. Alloys Compd.* **2018**, *762*, 398–408. [CrossRef]